Negative-Muon Spin Rotation at the Oxygen Site in Paramagnetic MnO†

S. Nagamiya, K. Nagamine, O. Hashimoto,* and T. Yamazaki

Department of Physics, Faculty of Science, University of Tokyo, Hongo, Bunkyo-ku, Tokyo, Japan,
and Lawrence Berkeley Laboratory, University of California, Berkeley, California 94720
(Received 5 May 1975)

Negative-muon spin rotation at the oxygen site in paramagnetic MnO has been observed at room temperature. A paramagnetic shift of $(1.16 \pm 0.21)\%$ was observed, approximately one-third the shift observed for the ^{17}O NMR in MnO. The muon-spin relaxation time extrapolated to zero external field was determined to be $1.5^{+0.8}_{-0.4}$ μsec. Possible mechanisms for explaining these observations are presented.

The negative muon (μ^-) is a new probe in the study of solid-state physics.[1] If μ^- is bound to a spinless nucleus, the muon-nucleus system (the ground-state muonic atom) is a pure magnetic probe because its spin is $\frac{1}{2}$. The bound-muon spin is polarized up to about 17%, which causes an asymmetric angular distribution of electrons decaying from the muons, and thus the muon spin rotation in the presence of magnetic field can be detected from a time distribution of decay electrons.

In this Letter we report observation of negative-muon spin rotation at the oxygen site in paramagnetic MnO. The oxygen atom in this magnetic oxide plays an important role in the superexchange interaction which gives rise to antiferromagnetic ordering of Mn^{2+} d electrons below $T_N = 116$ K.[2] Since μ^-O has a lifetime of 1.8 μsec, which is much longer than the lifetime of μ^-Mn (~ 0.2 μsec), the muon signal from oxygen can be selectively separated. Furthermore, the μ^--spin-rotation method may reveal new phenomena, since the μ^-O probe behaves as a nitrogenlike impurity (but with rather broader magnetization distribution as compared with the nitrogen nucleus). In order to study how the μ^-O probe is useful for the study of magnetic oxide and how this probe is different from the ^{17}O NMR probe, we started our measurements with paramagnetic MnO, since it is the exceptional case where the ^{17}O NMR has been observed.[3] Goals of our work are (a) to determine the paramagnetic shift (Δ) and spin relaxation time (T_2) of muons at oxygen sites, and (b) to compare these with the ^{17}O NMR data.

The experimental setup and the procedure of measurements were the same as those reported before.[1,4] Negative muons from the 184-in. cyclotron at Lawrence Berkeley Laboratory (LBL) were stopped at the rate of 10^3 sec^{-1} in a target of single-crystal MnO (3 cm×4 cm×5 g/cm^2; made by Nakazumi Crystal Co.). An external

magnetic field (6.830 and 1.1061 kOe) was applied on the target perpendicular to the beam direction. A (100) axis of MnO was parallel to the field. Temperature was ~ 300 K at which the MnO was in the paramagnetic phase.

The time spectrum of decay electrons from muons, as shown in Fig. 1(a), involves two decay components with lifetimes of 232 ± 3 nsec and 1.84 ± 0.02 μsec, which are in good agreement with the known lifetimes[5] of μ^-Mn and μ^-O, respectively. Since the muon spin associated with the Mn nucleus is expected to be depolarized rapidly enough, we have subtracted the short-lived component and analyzed the long-lived component only, which gives information on muons at oxygen sites in MnO.

The time spectrum of the long-lived component will be expressed by

$$N(t) = N_0 \exp(-t/\tau)$$
$$\times [1 + A \exp(-t/T_2) \cos(2\pi f + \varphi)], \quad (1)$$

where $\tau = 1.84 \pm 0.02$ μsec, A is the asymmetry, T_2 is the relaxation time, and f is the Larmor frequency. Figure 1(b) shows χ^2 fits for this long-lived component at $H = 6.830$ kOe as a function of f. The χ^2's have a sharp minimum at $f = 93.57 \pm 0.19$ MHz. The χ^2 fits for a carbon target under the same condition, as shown also in Fig. 1(b), gave a minimum at $f_0(\mu^-C) = 52 \pm 0.04$ MHz. After a small correction for the difference of the muon g factors between oxygen and carbon,[6] we have a paramagnetic shift Δ of μ^-O in MnO of

$$\Delta \equiv \delta H/H = (1.16 \pm 0.21)\%. \quad (2)$$

The value of Δ determined at $H = 1.1061$ kOe [$(0.9 \pm 0.8)\%$] involves larger error but is in agreement with the above value (2).

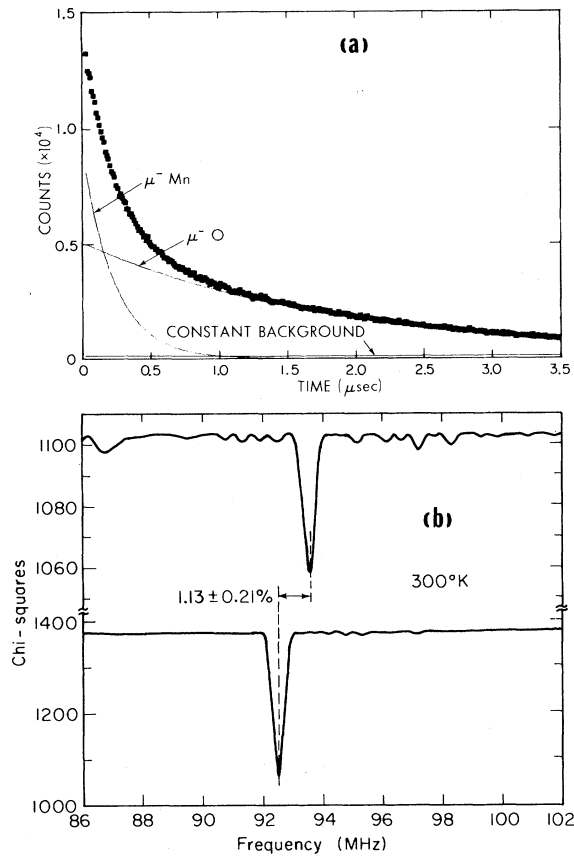The relaxation time T_2 has also been determined by χ^2 fits. Results are $0.7^{+0.7}_{-0.3}$ μsec at H

FIG. 1. (a) Time spectrum of decay electrons from the muons stopped in a MnO target. The long-lived component comes from $\mu^- O$ and the short-lived one from $\mu^- Mn$. (b) χ^2 versus the Larmor frequency for the $\mu^- O$ component in paramagnetic MnO at room temperature and at $H = 6.830$ kOe (upper part) and for a carbon target under the same experimental conditions (lower part), showing a paramagnetic shift of $(1.16 \pm 0.21)\%$ after the correction for the g-factor difference between $\mu^- O$ and $\mu^- C$.

$= 6.830$ kOe and $1.3^{+0.7}_{-0.3}$ μsec at $H = 1.1061$ kOe. By extrapolating these two values to zero external field, like the case of the ^{17}O NMR,[3] we obtain

$$T_2 = 1.5^{+0.8}_{-0.4} \ \mu\text{sec (at } H = 0). \tag{3}$$

The asymmetry A obtained from the best fits is around 3%.

We have carefully examined possible effects of long-lived background from muons stopped in the surrounding plastic counters, since its lifetime is around 1.8 μsec. From measurements on various other targets we have learned that the long-lived background has a precession frequen-

cy equal to $f_0(\mu^- C)$ with amplitude less than 1.5%. To test the effect of this background on $f(\mu^- O$ in MnO), therefore, we have added a time spectrum of $\mu^- C$ to the time spectrum of μ^- in MnO, and analyzed the frequency distribution of this superposed time spectrum. Two prominent peaks appear in the frequency spectrum, one at $f_0(\mu^- C)$ and the other at $f(\mu^- O$ in MnO), the latter being unchanged from the value given above ($f = 93.57 \pm 0.19$ MHz). Thus, we have finally found that the experimental value (2) is free from the effect of the long-lived background. The fact that the χ^2 fits for $\mu^- O$ in MnO shown in Fig. 1(b) have no peaks at around $f_0(\mu^- C)$ may indicate that the long-lived background was relatively small in the present measurements.

The present results are summarized and compared with the NMR data in Table I. The paramagnetic shift for $\mu^- O$ is approximately one-third the shift observed for the ^{17}O NMR. It is interesting to compare $g^2 T_2$ for $\mu^- O$ and ^{17}O, since the relaxation rate is proportional to g^2. As shown in column 5 of Table I, $g^2 T_2$ for $\mu^- O$ turns out to be one order of magnitude larger than $g^2 T_2$ for ^{17}O.

The paramagnetic shift is expressed as[3]

$$\Delta = - (6 \langle S_z \rangle / H) H_{hf}/S - 3\chi H_{hf}/S, \tag{4}$$

where $\langle S_z \rangle$ is the thermal average of the six neighboring Mn^{2+} spins ($S = \frac{5}{2}$) in the presence of an external field H, χ is the atomic susceptibility, and H_{hf} is the local hyperfine field at the oxygen site exerted from one neighboring Mn^{2+} spin,

$$H_{hf} = f_s (8\pi/3) \mu_B |\psi_{2s}(0)|^2. \tag{5}$$

Here f_s is the effective fractional occupancy by unpaired spins of $2s$ orbitals at the oxygen site.[2,3] The relaxation rate at the high-temperature limit which is subject to exchange narrowing is written as

$$\frac{1}{g^2 T_2} = 4 \left(\frac{\pi}{2}\right)^{1/2} \frac{S+1}{S} \frac{(\mu_N H_{hf}/\hbar)^2}{\omega_e}, \tag{6}$$

where ω_e, the exchange frequency, is related to the exchange integral J as follows[7]:

$$\omega_e = [2S(S+1)/3]^{1/2} J/\hbar. \tag{7}$$

Assuming χ and ω_e constant, we would expect a "Korringa-type" relation,

$$\Delta^2 g^2 T_2 = \text{const}, \tag{8}$$

which is consistent with the experimental observations (see column 6 of Table I). Thus, this simple-minded consideration would indicate that

TABLE I. Summary of the paramagnetic shift Δ and relaxation time T_2 observed at room temperature by different methods for paramagnetic MnO. The relaxation times have been obtained from extrapolation of experimental data to zero external magnetic field

Probe	g factor (μ_N)	Δ (%)	T_2 (μsec)	$g^2 T_2$ ($10^2 \mu$sec)	$\Delta^2 g^2 T_2$ ($10^{-2} \mu$sec)	Ref.
$\mu^- O$	17.76^a	1.16 ± 0.21	$1.5^{+0.8}_{-0.4}$	$4.7^{+2.5}_{-1.3}$	$6.4^{+3.7}_{-1.8}$	present
^{17}O	-0.7575	3.21 ± 0.02	74 ± 26	0.42 ± 0.15	4.4 ± 1.6	3

$^a g(\mu^- O)$ measured in nonmagnetic substance (Ref. 6).

$H_{hf}(\mu^- O)$ is one-third of $H_{hf}(^{17}O)$.

For further interpretation of the experimental results, however, a more detailed analysis has to be done. First of all we should recognize that the $\mu^- O$ probe behaves like a dilute N^{3-} impurity at the oxygen site in MnO. The only difference between $\mu^- O$ and N^{3-} lies in the spatial distribution of the probe: The N nucleus has a sharply cut-off radius with $R = 2$ fm while $\mu^- O$ has a broad exponential-type distribution with a Bohr radius of ~ 30 fm. However, since the latter is still 200 times smaller than the electron Bohr radius, we ignore a possible hyperfine anomaly[8] in the following discussions.

(1) Using a recent Hartree-Fock calculation[9] for Na^+, Ne, F^-, O^+, O, O^-, N^+, N, and N^-, we estimated $|\psi_{2s}(0)|^2_{O^{2-}} = 44 \times 10^{24}$ cm^{-3} and $|\psi_{2s}(0)|^2_{N^{3-}} = 26 \times 10^{24}$ cm^{-3}, and thus $|\psi_{2s}(0)|^2_{N^{3-}} / |\psi_{2s}(0)|^2_{O^{2-}} = 0.6$, which is certainly a part of the origin of the observed reduction in H_{hf}.

(2) The excess negative charge of $\mu^- O$ compared to ^{17}O will push out $2p$ and $2s$ electrons farther from the oxygen site, which will increase the local metal-oxygen covalency ($2p$-$3d$ and $2s$-$3d$ mixtures). Since f_s is related to the covalency parameter λ_s and the overlap S_s between $2s$ and $3d$ through the expression $f_s = (S_s + \lambda_s)^2$,[3] it is expected that $f_s(\mu^- O) > f_s(^{17}O)$. This sets a lower limit 0.6 on $H_{hf}(\mu^- O)/H_{hf}(^{17}O)$, which cannot account for the observed reduction in Δ. This conclusion might be altered if the $1s$-electron polarization plays a significant role in H_{hf}, but the following point seems to be more important.

(3) So far we have neglected the possible difference in $\langle S_z \rangle$ and ω_e between $\mu^- O$ and ^{17}O. However, since the presence of $\mu^- O$ increases the local covalency and thus enhances the local superexchange interaction, $\langle S_z \rangle$ and ω_e in Eqs. (4) and (6) should now be read as the local average $\langle S_z \rangle$ (which can be named local susceptibility) and local exchange frequency. If the enhanced superexchange interaction causes an increase of the local Weiss temperature Θ ($\Theta \propto J/k$), and Θ is still related to χ by

$$\chi \propto 1/(T + \Theta), \tag{9}$$

the local χ would be smaller than the bulk susceptibility. Considering that $H_{hf}(\mu^- O) > 0.6 H_{hf}(^{17}O)$, we would obtain $\Theta_{local} > 2000$ K in order to account for $\Delta(\mu^- O)$, while $\Theta_{bulk} = 610$ K. Obviously the observed relaxation time would require that the local exchange frequency should increase in accordance with the relation

$$\omega_e \propto \Theta. \tag{10}$$

If such a situation is real, the temperature dependence of $\Delta(\mu^- O)$ will be different from that of χ_{bulk}, but this point is open to further experimental studies.

[1]T. Yamazaki, K. Nagamine, S. Nagamiya, O. Hashimoto, K. Sugimoto, K. Nakai, and S. Kobayashi, to be published, and in Proceedings of the International Conference on Hyperfine Interactions Studied by Nuclear Reactions and Decays, Uppsala, Sweden, 1974, edited by E. Karlsson and R. Wappling (Univ. of Uppsala, Upp-

sala, Sweden, 1974).

[2]See, for instance, P. W. Anderson, in *Solid State Physics*, edited by H. Ehrenreich, F. Seitz, and D. Turnbull (Academic, New York, 1963), Vol. 14, p. 99.

[3]D. E. O'Reilly and T. Tsang, J. Chem. Phys. 40, 734 (1964).

[4]T. Yamazaki, S. Nagamiya, O. Hashimoto, K. Nagamine, K. Nakai, K. Sugimoto, and K. M. Crowe, Phys. Lett. 53B, 117 (1974).

[5]G. Feinberg and L. M. Lederman, Annu. Rev. Nucl. Sci. 13, 431 (1963).

[6]D. P. Hutchinson, J. Menes, G. Shapiro, A. M. Patlach, and S. Penman, Phys. Rev. Lett. 7, 129 (1961), and Phys. Rev. 131, 1362 (1963).

[7]T. Moriya, Progr. Theor. Phys. 16, 23, 641 (1956).

[8]A. Bohr and V. F. Weisskopf, Phys. Rev. 77, 94 (1950). See also H. H. Stroke, R. J. Blin-Stoyle, and V. Jaccarino, Phys. Rev. 123, 1326 (1961); H. J. Rosenberg and H. H. Stroke, Phys. Rev. A 5, 1992 (1972).

[9]E. Clementi and C. Roetti, At. Data Nucl. Data Tables 14, 177 (1974).

Droplet Model of Electron-Hole Liquid Condensation in Semiconductors*

T. L. Reinecke†

Naval Research Laboratory, Washington, D. C. 20375

and

S. C. Ying‡§

Laboratoire de Physique des Solides, Université Paris-Sud, Orsay, France

(Received 24 February 1975)

A model based on noninteracting droplet fluctuations is used to describe the phase diagram for electron-hole liquid condensation in semiconductors. All liquid and gas densities are related to the liquid density at low T. Good agreement is obtained by fitting recent detailed measurements of the phase diagram for Ge, and an experimental estimate of droplet surface tension ($\sim 1.0 \times 10^{-4}$ erg/cm^2) is obtained. Theoretical values of the critical temperature and density for Ge are given. A theoretical phase diagram for Si is presented.

The condensation of high-density nonequilibrium carriers into electron-hole–liquid (EHL) droplets in Ge and Si at low temperatures has been studied extensively both experimentally[1-3] and theoretically.[4,5] The liquid-gas phase diagram provides an especially full picture of the condensation (see Fig. 1): It is the boundary (in density-temperature) separating a "gas" of excitons, electrons, and holes from the high-density "metallic-liquid" phase and a coexistence region (characterized by droplets of EHL). The most detailed experimental studies have been made for Ge. Thomas *et al.*[6] have recently measured the entire phase diagram for Ge, especially the region near the critical temperature, T_c. Their results are given in Fig. 1.

FIG. 1. Phase diagram in temperature and density of electrons and holes in Ge. The experimental points are from Ref. 6; the solid curve is obtained from the droplet model using parameters given in text; $\rho_{s.p.}$ gives the temperature dependence of the liquid density due to single-particle excitations, and is obtained from the experimental results.